Engineering of a dual-periodic optical superlattice used in a coupled optical parametric interaction

Zhao-Wei Liu, Yan Du, Jun Liao, Shi-Ning Zhu, Yong-Yuan Zhu, Yi-Qiang Qin, Hui-Tian Wang, Jing-Liang He, Chao Zhang, and Nai-Ben Ming

National Laboratory of Solid State Microstructures, Nanjing University, Nanjing 210093, China

Received November 13, 2001; revised manuscript received January 7, 2002

Quasi-phase matching facilitates the phase matching of any parametric interaction by setting an appropriately modulated period. We propose a dual-periodic structure that is used in the construction of a frequency-conversion device. For example, we have designed and fabricated such a dual-periodic structure in a $LiTaO_3$ crystal. Using a fundamental source at 1.064 μm, we obtained ultraviolet radiation at 355 nm and green radiation at 532 nm simultaneously by frequency tripling and frequency doubling the fundamental source. Theoretically, this idea can be further extended to the design of a multiperiodic structure for achievement of more quasi-phase-matched processes in a single optical superlattice. © 2002 Optical Society of America

OCIS codes: 190.2620, 190.4160, 220.4000.

1. INTRODUCTION

Since quasi-phase matching (QPM) was devised independently by Armstrong *et al.*[1] and by Franken and Ward,[2] the theory of QPM has been useful in the realm of periodic optical superlattices and has opened a novel research field in nonlinear optics. Based on the theory of QPM, periodic domain structure has wide applications not only for second-harmonic generation (SHG),[3–5] sum-frequency generation (SFG),[6] difference-frequency generation,[7] and optical parametric oscillators[8] but also for new fields such as generation of squeezed light for optical communication and information processing[9] and optical solitons.[10] At the same time, efforts have been concentrated on finding the potential applications of quasi-periodic optical superlattices[11–15] (QPOSs) in coupled optical parametric processes.

Although it gives a complete solution of the phase-matching problem for any specific interaction, the periodic structure generally fails to solve the problem for some efficient coupled interactions. Coupled interaction consists of two or more separate but cascaded parametric processes. The achievement of efficient coupled interaction requires that all parametric processes be phase matched simultaneously in a superlattice crystal. Although a periodic structure may provide a set of reciprocals for QPM interactions, it generally fails to provide such a set of reciprocals simultaneously for each different QPM interaction because its reciprocals are all integral multiples of the primitive vector, whereas the crystal's dispersion depends nonlinearly on the frequency.

To solve this problem, Zhu *et al.* proposed application of a quasi-periodic structure to a QPM coupled parametric process because such a structure has plentiful reciprocals and the ratio of different reciprocals is irreducible. The first experimental realization of the QPM coupled parametric process of which we are aware was achieved in 1997.[11] In that demonstration, efficient third-harmonic green light was generated in a Fibonacci optical superlattice of $LiTaO_3$ (LT) by coupling of SHG and SFG. Since then, various kinds of complex structure, including Fibonacci,[12–14] Thue–Morse,[16] intergrowth,[17] and aperiodic[18] structures, have been explored. Multiple-peak frequency doubling and quadrupling with a single crystal with a structure sequence that coincidentally phase matches several processes simultaneously at some fundamental wavelength were also demonstrated.[19] The same problem was ultimately solved recently in a general two-component quasi-periodic structure by the projection method proposed by Zhang *et al.*[20] and Keren *et al.*[13] In this structure one selects the ratio of reciprocals by changing the projection angle such that the structure can simultaneously provide two reciprocals to compensate for phase mismatching of two separate parametric processes, which makes the processes quasi-phase matched. Therefore quasi-phase-matched third-harmonic generation (THG) can be attained in the superlattice for an arbitrary fundamental wavelength.

In this paper we introduce another novel structure, a dual-periodic structure, in which two optical parametric interactions are coupled into a single superlattice crystal. Compared with other structures, this one provides clearer physical sight into and great design flexibility for quasi-phase-matched coupled parametric processes. The design of this structure can be achieved in both real space and reciprocal space for a typical coupled parametric process, i.e., THG. For example, we designed and fabricated such a dual-periodic domain-reversal structure in a LT crystal, and the primary experimental result was presented at the same time.

0740-3224/2002/071676-09$15.00

2. THEORY

A. Wave Equations Describing Third-Harmonic Generation

It is well known that generation of high-order harmonics requires cascading a couple of second-order nonlinear interactions, such as THG, which is generated through two processes, SHG and SFG. Traditionally, these two processes are achieved in two homogeneously nonlinear crystals or in two separate optical superlattices. In this paper we demonstrate that THG can be efficiently achieved in a dual-periodic superlattice by a coupled parametric process. The following equations describe the processes mentioned above:

$$\begin{aligned}\frac{dA_1}{dx} &= i\kappa_2 A_3 A_2^* \exp(-i\Delta k_2 x) \\ &\quad - i\kappa_1 A_2 A_1^* \exp(-i\Delta k_1 x), \\ \frac{dA_2}{dx} &= -i\kappa_2 A_3 A_1^* \exp(-i\Delta k_2 x) \\ &\quad - \frac{i}{2}\kappa_1 A_1^{\,2} \exp(i\Delta k_1 x), \\ \frac{dA_3}{dx} &= -i\kappa_2 A_1 A_2 \exp(i\Delta k_2 x),\end{aligned} \tag{1}$$

where wave amplitude $A_i = (n_i/\omega_i)^{1/2} E_i$ $(i = 1, 2, 3)$ represent the fundamental, the second harmonic (SH), and the sum frequency (SF), respectively; Δk_1 and Δk_2 are the wave-vector mismatches of SHG and SFG, respectively, and

$$\begin{aligned}\Delta k_1 &= k^{2\varpi} - 2k^{\varpi} - G_{m,n}, \\ \Delta k_2 &= k^{3\varpi} - k^{2\varpi} - k^{\varpi} - G_{m',n'},\end{aligned} \tag{2}$$

where k_1, k_2, and k_3 represent the wave vectors of the fundamental, the SH, and the SF and $G_{m,n}$ and $G_{m',n'}$ are the reciprocals of the superlattice. κ_1 and κ_2 in Eqs. (1) are two coupling coefficients, and they are represented as follows:

$$\begin{aligned}\kappa_1 &= \frac{d_{m,n}}{c}\left(\frac{\omega_2 \omega_1^{\,2}}{n_2 n_1^{\,2}}\right)^{1/2} \\ \kappa_2 &= \frac{d_{m',n'}}{c}\left(\frac{\omega_3 \omega_2 \omega_1}{n_3 n_2 n_1}\right)^{1/2},\end{aligned} \tag{3}$$

where n_1, n_2, n_3, and ω_1, ω_2, ω_3 are the refractive indices and the angular frequencies of the fundamental, the SH, and the third harmonic (TH), respectively, and c is the speed of light in free space. κ_1 and κ_2 are proportional to the effective nonlinear coefficients of superlattices $d_{m,n}$ and $d_{m',n'}$, and m, n and m', n' are integers. In theory, it has been verified that efficient quasi-phase matched THG depends not only on the magnitude of these two coupling coefficients but also on their ratios.[21] The ratio determines the ultimate energy distribution among the three waves. For THG there are following boundary conditions: $A_1(0) = A_{10}$, $A_2(0) = 0$, and $A_3(0) = 0$. In Eqs. (1) there are five distinct parametric processes: one SH, one SF, and three difference-frequency processes. If Δk_1 and Δk_2 are not equal to zero, these five parametric interactions and their coupling are relatively weak and the energy of fundamental cannot be efficiently transferred to the SH and the TH. If, however, $\Delta k_1 = \Delta k_2 = 0$, that is, if two QPM conditions of SHG and SFG are satisfied simultaneously, the situation will be quite different: Five parametric processes all can proceed efficiently, and the coupling of the three waves will be greatly enhanced. The energy conversion can efficiently proceed in the superlattice.

B. Achievement of Third-Harmonic Generation in a Dual-Period Optical Superlattice

From what has been discussed above, the most important way to achieve highly efficient THG is to construct a structure that may provide two reciprocals to compensate for the mismatches of SHG and SFG and make these two processes quasi-phase matched. One can obtain the required reciprocals by designing an appropriate domain-inverted sequence in a superlattice. Fourier transformation is a method in common use for analysis of the distribution of reciprocals and their magnitudes in wave-vector space. The Fourier spectrum of a one-dimensional periodic optical superlattice (POSL) can be written as

$$F_{\mathrm{POSL}}(x) = \sum_m f_m \exp(iG_m x), \tag{4}$$

with reciprocals

$$G_m = 2\pi m/\Lambda, \qquad m = 1, 2, 3 \ldots \tag{5}$$

and Fourier coefficients

$$f_m = \frac{2}{m\pi}\sin\left(\frac{m\pi}{2}\right). \tag{6}$$

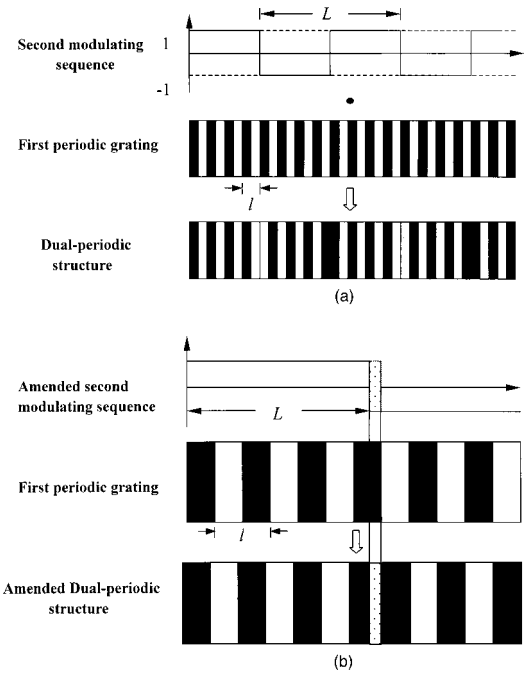

Fig. 1. Dual-period QPM structure formed by modulation twice upon a periodic grating. (a) Ratio L/l is an integer. (b) Amended method for obtaining a dual-periodic structure with the ratio of l to L unmeasurable.

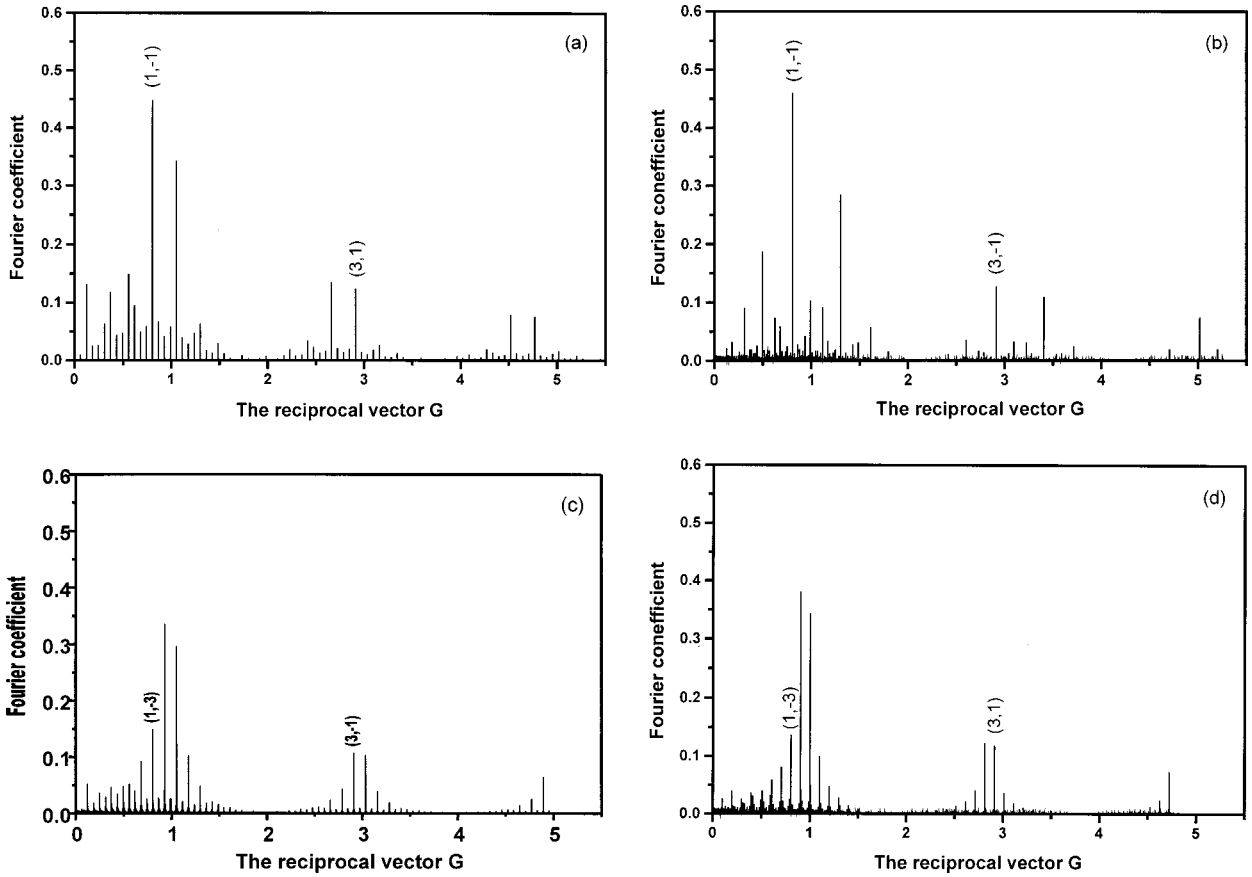

Fig. 2. Fourier spectrum of the four dual-periodic structures. The two reciprocals marked are used for SHG and SFG (left to right).

Equation (5) shows that a periodic structure can provide a set of reciprocals (G_m, $m = 1, 2, 3 \ldots$) in which each is an integer of a primitive vector G_1. The structure's magnitude, Fourier coefficient f_m, is in proportion to the corresponding effective nonlinear coefficient of the periodic structure, $d_m = f_m d$, where d is the nonlinear coefficient of the crystal. Generally, the ratio of wave-vector mismatches of SFG and SHG is not an integer owing to dispersion, so the periodic structure seldom satisfies the general QPM conditions of SHG and SFG simultaneously.

To solve the problem we propose using a general two-component quasi-periodic optical superlattice (QPOSL). This one-dimensional quasi-periodic structure may be considered the projection of a two-dimensional square structure on a straight line, and the arrangement of its two elementary components depends on projection angle θ. The sequence and therefore its reciprocals can be changed through adjustment of angle θ. The Fourier spectrum of this structure is

$$F_{\mathrm{QPOSL}}(x) = \sum_{m,n} f_{m,n} \exp(iG_{m,n}x), \tag{7}$$

with reciprocals

$$G_{m,n} = \frac{2\pi(m + n\tau)}{D} \tag{8}$$

and Fourier coefficients

$$f_{m,n} = 2\frac{(1 + \tau)l}{D} \frac{\sin(G_{m,n}l/2)}{G_{m,n}l/2} \frac{\sin(X_{m,n})}{X_{m,n}}, \tag{9}$$

$$X_{m,n} = \pi D^{-1}\tau^2(ml_A - nl_B), \tag{10}$$

$$D = \tau l_A + l_B; \tag{11}$$

m and n are integers; D is an average structural parameter; l_A and l_B are two elementary components, and both consist of a pair of inverse polarizations; l presents the width of positive polarization in l_A and l_B; and $\tau = \tan\theta$ is an adjustable parameter. Because the quasi-periodic structure has more-abundant reciprocals than the periodic structure has, and among them there are two reciprocals that one can independently design by changing projection angle θ, QPM can be simultaneously achieved in two different parametric processes, such as SHG and SFG, in the same quasi-periodic optical superlattice.

A dual-periodic structure was introduced into a superlattice based on a similar object. It permits more flexibility in the choice of reciprocals than does a quasi-periodic structure. The dual-periodic structure is formed by twice-periodic modulation. We label these two modulated periods l and L, where $l < L$ [Fig. 1(a)]. Two periodically modulated sequences, $F_1(x)$ and $F_2(x)$, can be extended into two Fourier series:

$$F_1(x) = \sum_{m=-\infty}^{\infty} f_m \exp(-iG_m x),$$

$$F_2(x) = \sum_{n=-\infty}^{\infty} f_n \exp(-iG_n x). \tag{12}$$

Therefore the dual-periodic structure can be written as

$$\begin{aligned} F(x) &= F_1(x)F_2(x) \\ &= \sum_{m,n=-\infty}^{\infty} f_m f_n \exp[-i(G_m + G_n)x] \\ &= \sum_{m,n=-\infty}^{\infty} f_{mn} \exp(-iG_{m,n}x), \end{aligned} \tag{13}$$

where $G_{m,n} = G_m + G_n$ and $f_{m,n} = f_m f_n$. Thus the reciprocals of this dual-periodic structure can be expressed as

$$G_{m,n} = G_m + G_n = mG_l + nG_L, \tag{14}$$

where $G_l = 2\pi/l$ and $G_L = 2\pi/L$ are the first-order reciprocals of these two modulated periods. Integers m and n label the order of reciprocals. Because these two periods, l and L, are independent of each other, the structure can provide two independent reciprocals to compensate for the phase mismatches of two different parametric processes, making them simultaneously quasi-phase matched.

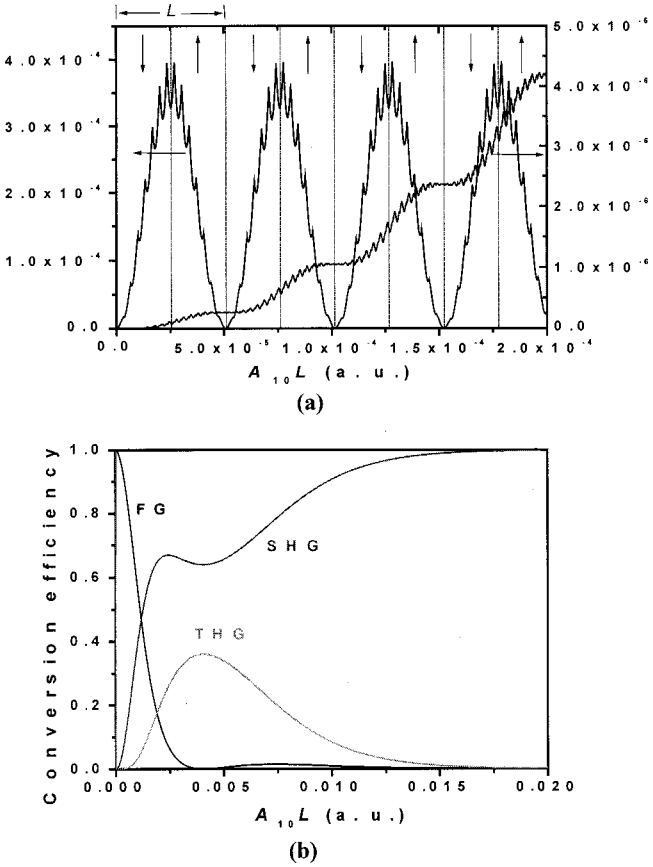

Fig. 3. (a) Evolution of the three waves in a dual-periodic structure. The larger period L of the dual-periodic structure is marked at the top. (b) Efficiencies of SHG and THG versus $A_{10}L$ in a periodic structure (period $l = 6.77\ \mu$m, $L = 50.86\ \mu$m).

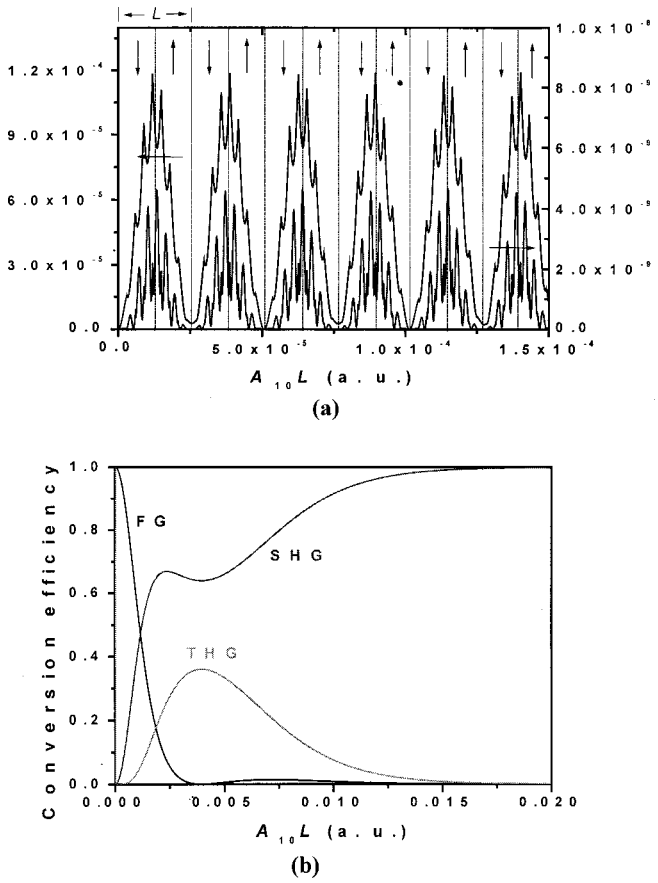

Fig. 4. Same as in Fig. 3, except that here $l = 5.67\ \mu$m and $L = 25.42\ \mu$m.

C. Third-Harmonic Generation in a Dual-Periodic Optical Superlattice

Here we show how to achieve THG in a dual-periodic optical superlattice (DPOSL). The third-harmonic can be generated by coupling of SHG and SFG in a quadric nonlinear medium; therefore the QPM condition for THG in a DPOSL for collinear interaction is

$$\Delta k_1 = k_2 - 2k_1 - G_{m,n} = 0 \tag{15}$$

for SHG and

$$\Delta k_2 = k_3 - k_2 - k_1 - G_{m',n'} = 0 \tag{16}$$

for SFG, where $G_{m,n}$ and $G_{m',n'}$ are two predesigned reciprocals of the DPOSL. According to Eqs. (14)–(16),

$$G_{m,n} = mG_l + nG_L = \frac{4\pi}{\lambda}(n_2 - n_1) = \frac{2\pi m}{l} + \frac{2\pi n}{L},$$

$$\begin{aligned} G_{m',n'} &= m'G_l + n'G_L = \frac{2\pi}{\lambda}(3n_3 - 2n_2 - n_1) \\ &= \frac{2\pi m'}{l} + \frac{2\pi n'}{L}. \end{aligned} \tag{17}$$

Here λ is the fundamental wavelength, and n_1, n_2, and n_3 are the refractive indices of the fundamental, the SH, and the TH, respectively, of the nonlinear crystal. m' and n' are integers like m and n.

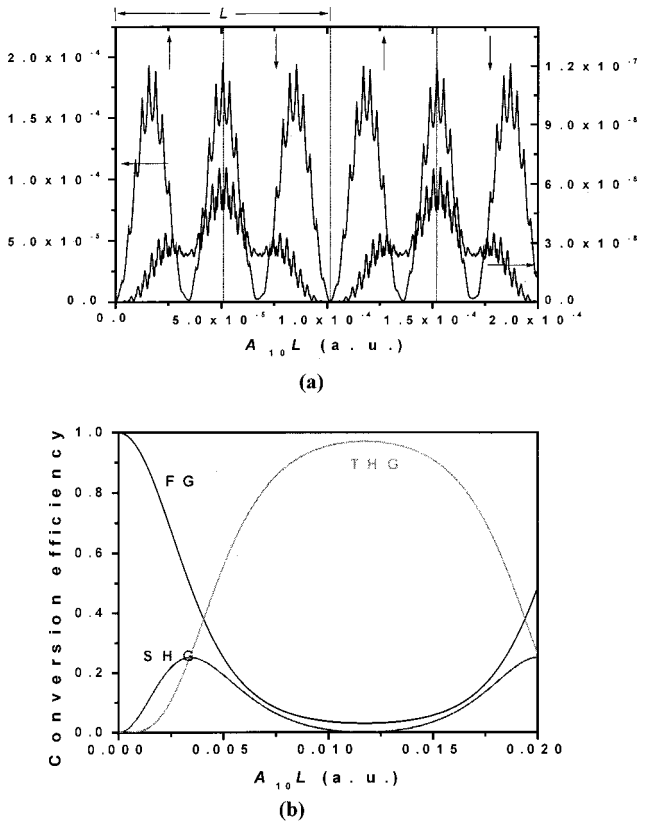

Fig. 5. Same as in Fig. 3, except that here $l = 6.34\ \mu$m and $L = 101.67\ \mu$m.

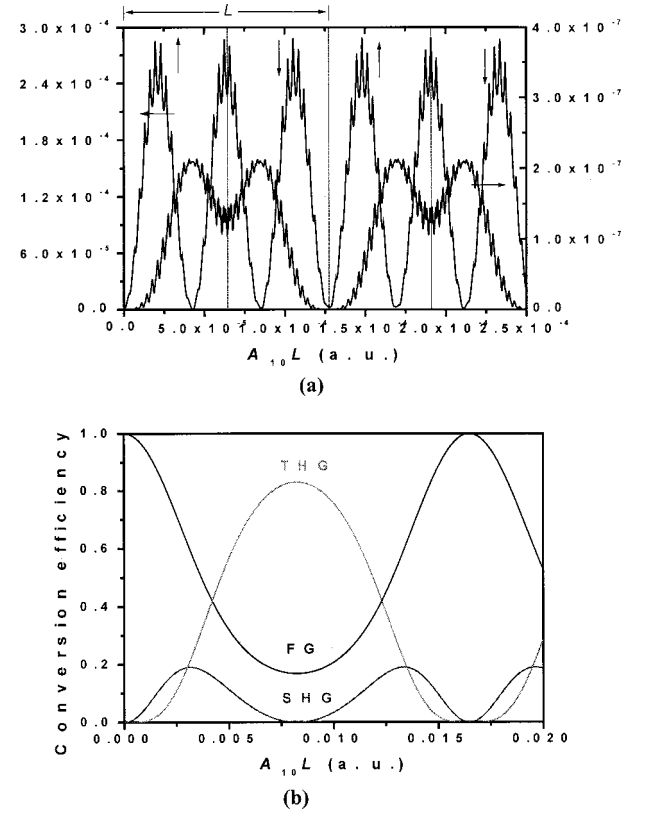

Fig. 6. Same as in Fig. 3, except that here $l = 6.58\ \mu$m and $L = 127.08\ \mu$m.

If the fundamental wavelength is chosen to be a specific wavelength by selection of appropriate values of m, n, m', and n' one can determine the two main parameters of the dual-periodic structure (l and L) from Eqs. (14)–(16). Here a THG of 1064 nm in a LT DPOSL is shown. All parameters are designed for a phase-matching temperature of 50 °C.

Without loss of generality, we select various values of m, n, m', and n', consisting of four sets of different dual-periodic structure. They are (a) $m = 1$, $n = -1$, $m' = 3$, $n' = 1$, $l = 6.77\ \mu$m, and $L = 50.86\ \mu$m; (b) $m = 1$, $n = -1$, $m' = 3$, $n' = -1$, $l = 5.67\ \mu$m, and $L = 25.42\ \mu$m; (c) $m = 1$, $n = -3$, $m' = 3$, $n' = -1$, $l = 6.34\ \mu$m, and $L = 101.67\ \mu$m; and (d) $m = 1$, $n = -3$, $m' = 3$, $n' = 1$, $l = 6.58\ \mu$m, and $L = 127.08\ \mu$m. Fourier spectra of these structures are shown in Fig. 2. We can see that the heights of the two reciprocal vectors are unequal when $m = n$ and $m' = -n'$ because of the shift of the second modulated sequence to one direction. The evolutions of the three waves in these four structures in Figs. 2(a), 2(b), 2(c), and 2(d) are shown in Figs. 3(a), 4(a), 5(a), and 6(a), respectively. Some parameters of these four structures are listed in Table 1. We can see that the maximum conversion efficiency of THG in Fig. 5(b) is higher than the others because the ratio (1.388) of the corresponding two Fourier coefficients is closer than the others to the optimum ratio (1.464).[21] However, it is obvious that the conversion speed of the TH is slower than those for the other cases at a low input power or for a short sample lengths. Therefore, for high THG efficiency the selection of structure parameters should be related to the crystal length and the power density of the fundamental wave. The situation may occur in any three-wave coupling parametric process. The result shows that a DPOSL provides additional feasibility for high THG efficiency because of its improved structure design.

We can also analyze the coupled parametric process in real space to get the spatial variation of the conversion efficiency. Figure 7 shows the spatial variations of SH and TH intensities for phase mismatching in a homogeneous crystal. It can be seen that alternating the sign of the power flow leads to repetitive growth and decay of the SH and the SH intensities along the length of the interaction. Obviously the conversion coefficients of SHG and THG here are low. The half-period of fluctuation is called the coherence length. If the superlattice is a periodic structure and its period is equal to twice the coherence length of SHG, the QPM condition for SHG is satisfied. In other words, efficient SHG can be achieved in a single periodic domain-inverted structure. In this case the output of THG still fluctuates spatially as a result of the phase mismatching of SFG processes, however, the period of fluctuation increases and is longer than that in a homogeneous crystal (as shown in Fig. 7). Practically, the design of a DPOSL for THG has the following two steps: In the first step we fix the two phase mismatches of SHG and SFG at the same magnitude, that is, $\alpha\Delta k_1 = \beta\Delta k_2$, where $\alpha, \beta = \pm 1, \pm 2, \pm 3 \ldots$, with a periodic structure l. In the second step we modulate the first periodic grating by using a longer period L [Fig. 1(a)], so the phase mis-

Table 1. Parameters of Four Dual-Periodic Superlattices and Their Relationship to One Another

l (μm)	L (μm)	Reciprocal Vector Used in SHG($G_{m,n}$)	Its Corresponding Fourier Coefficient ($f_{m,n}$)	Reciprocal Vector Used in THG($G_{m',n'}$)	Its Corresponding Fourier Coefficient ($f_{m',n'}$)	Ratio of the Two Fourier Coefficients ($f_{m,n}/f_{m',n'}$)	Figure That Shows the Evolution of the Three Waves
6.77	50.86	$G_{1,-1}$	0.4483	$G_{3,1}$	0.1242	3.610	3(a)
5.67	25.42	$G_{1,-1}$	0.4600	$G_{3,-1}$	0.1275	3.608	4(a)
6.34	101.67	$G_{1,-3}$	0.1487	$G_{3,-1}$	0.1071	1.388	5(a)
6.58	127.08	$G_{1,-3}$	0.1368	$G_{3,1}$	0.1186	1.153	6(a)

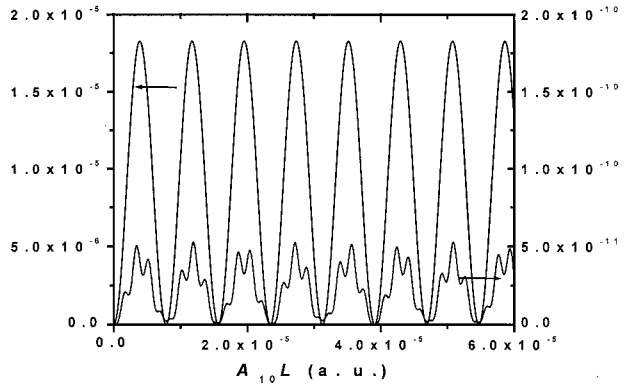

Fig. 7. Evolution of SHG and THG versus parameter $A_{10}L$ in a homogeneous LT crystal.

match of SHG and SFG can be compensated for simultaneously in an α-order QPM scheme and a β-order QPM scheme, respectively.

We take the four DPOSLs mentioned above as examples. First we choose a certain modulating periodic l based on $\alpha = 1$ and $\beta = -1$; thus, at every point where the integer time is l, the phase mismatches of these two processes have the same magnitude but opposite sign. The little peaks in the SHG curve correspond to the points where the nonlinear coefficient of the crystal changes its sign. The spatial variations of the conversion efficiencies of SHG and THG in the depleted fundamental are illustrated in Fig. 3(a). In this case the efficiency of SHG fluctuates with a long period L along the crystal length, and the efficiency of THG increases gradually like a set of stairs with the same period L. At every point of integer time L the mismatch of SHG and SFG has the same magnitude. By modulating a smaller structure with period L as shown in Fig. 3(a), one can correct the phase mismatches of SHG and SFG simultaneously. The resulting spatial variations of the conversion efficiencies of SHG and THG in the dual-periodic structure are displayed in Fig. 3(b). The ultimate pattern of the dual-periodic structure might be as shown in Fig. 1(a). The two main parameters of the dual-periodic structure are $l = 6.77$ μm and $L = 50.86$ μm. Because the ratio of l and L is usually unmeasurable, to avoid the appearance of a small amount of domain chirp one may adopt an amended method; that is, one may shift the boundary of each modulated sequence to the closest domain wall [Fig. 1(b)]. Therefore the mean value of the period of the modulating sequence is still equal to L although each modulating period is not exactly L.

Different dual-periodic structures can be induced through choice of various-order QPM schemes in SHG and SFG. For Fig. 4 we chose $\alpha = \beta = 1$ and $l = 5.67$ μm for the first periodic structure. The mismatch in SHG of first-order QPM is equal to that in SFG of third-order QPM in this periodic structure. The figure shows that the spatial evaluations of SHG and THG have the same period. Then by selecting this oscillation period as the second modulated period ($L = 25.42$ μm) we build a new dual-periodic structure. The relation of the conversion efficiency of SHG and THG to the crystal length in this dual-periodic structure is shown in Fig. 4(b). For Fig. 5 we chose $\alpha = 1$, $\beta = 3$, and $l = 6.34$ μm. In these conditions the mismatch in SHG of first-order QPM is three times of that in SFG of third-order QPM. The SHG and THG conversion efficiencies in the first period are structured as in Fig. 5(b). Modulating the first grating in the larger period L (101.67 μm) can compensate for the mismatch in the two processes simultaneously through third-order and first-order QPM, respectively. Figure 6 illustrates another case for which $\alpha = 1$, $\beta = -3$, $l = 6.58$ μm, and $L = 127.08$ μm, and the evolution of the three waves in this structure is shown in Fig. 6(a).

3. MULTIPERIODIC OPTICAL SUPERLATTICE EXTENDED FROM A DUAL-PERIODIC OPTICAL SUPERLATTICE

Based on a similar theory, the DPOSL can be extended to become a multiperiodical optical superlattice (MPOS), which is more flexible than a DPOS in the choice of reciprocals because of its more readily tunable parameters. Given a general definition of their similarity, a MPOS is fabricated by nth periodic modulation. The Fourier transform of each one of n periodically modulated sequences $F_j(x)$ can generally be expressed as a Fourier series:

$$F_j(x) = \sum_{m=-\infty}^{\infty} f_m{}^{(j)} \exp(-iG_m{}^{(j)}x) \qquad (j = 1, 2, 3 \ldots n). \tag{18}$$

Therefore the MPOS can be given as

$$\begin{aligned} F(x) &= F_1(x)F_2(x) \ldots F_n(x) \\ &= \sum_{m=-\infty}^{\infty} f_m{}^{(1)} f_m{}^{(2)} \ldots f_m{}^{(n)} \\ &\quad \times \exp[i(G_m{}^{(1)} + G_m{}^{(2)} + \ldots G_m{}^{(n)})x] \\ &= \sum_{m,n=-\infty}^{\infty} f_M \exp(-iG_M x), \end{aligned} \tag{19}$$

where $G_M = \Sigma_{i=1}^{n} G_m^{(i)}$ and $f_M = \Pi_{i=1}^{n} f_m^{(i)}$. The reciprocals of this multiperiodic structure can be expressed as

$$G_M = \sum_{i=1}^{n} G_{m_i}^{(i)} = \sum_{i=1}^{n} m_i G_{l_i}, \tag{20}$$

where l_i is the modulated period, and $G_{l_i} = 2\pi/l_i$ is the first-order reciprocal of every modulated period. Integers m_i label the order of reciprocals. In addition, periodic and quasi-periodic modulation can be mixed in the same structure in a similar way. More QPM processes can be expected to occur simultaneously in this MPOS.

4. EXPERIMENT

In a sample experiment we fabricated one kind of dual-periodic domain-reversal structure ($l = 6.77\ \mu$m, $L = 50.86\ \mu$m) in a z-cut LT wafer through an electric field that was poled at room temperature.[22,23] The sample had a thickness of ~0.5 mm and a total length of ~12 mm. An optical photograph of a LT DPOSL revealed by etching is shown in Fig. 8.

An infrared 1064-nm laser was generated from a Nd:YVO_4 crystal pumped by an 808-nm laser diode. Modulation with an acoustic-optical Q switch produced a quasi-cw laser with a pulse duration of 150 ns and a repetition rate of 13 kHz. The fundamental wave was focused into a beam, the radius of whose waist was ~0.2 mm, and coupled into the polished but uncoated end face of the sample. The focus of the lens was 50 mm. Both fundamental and harmonic waves were polarized along the z axis of crystal and transmitted along the x axis of the LT wafer. The sample was heated in a heater (Model OTC-PPLN-20, Super Optronics Ltd.) and tuned to the appropriate phase-matching temperature with an accuracy of 0.1 °C. We determined the nonlinear optical features of the sample by measuring the powers of the SH and the TH relative to the QPM temperature and input power of the fundamental.

Figure 9(a) shows the output of SHG and THG as a function of temperature. The phase-matching temperatures are located at 50.5 °C for SHG and at 49.0 °C for THG. At an average fundamental power of 1.1 W, the maximum output power of SHG and THG is 95 and 3.6 mW, respectively. Owing to Fresnel reflection of ~13% on the front surface of the sample, the actual fundamental average power transmitted into the sample was ~0.96 W. The fact that the SHG and THG peaks do not overlap may originate from the precise pattern of the lithographic mask or the deviation of the Sellmeier equation used for the LT crystal or both. Figure 9(b) shows that the SHG and THG power increases gradually with increasing fundamental power at the operating temperature of 49 °C. When the fundamental average power was tuned to 1.56 W, ~10 mW of UV light was generated. Because this

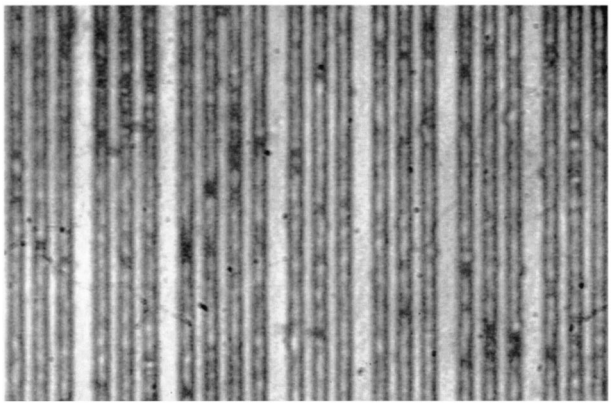

Fig. 8. Optical micrograph of a dual-periodic superlattice as revealed by etching ($+c$).

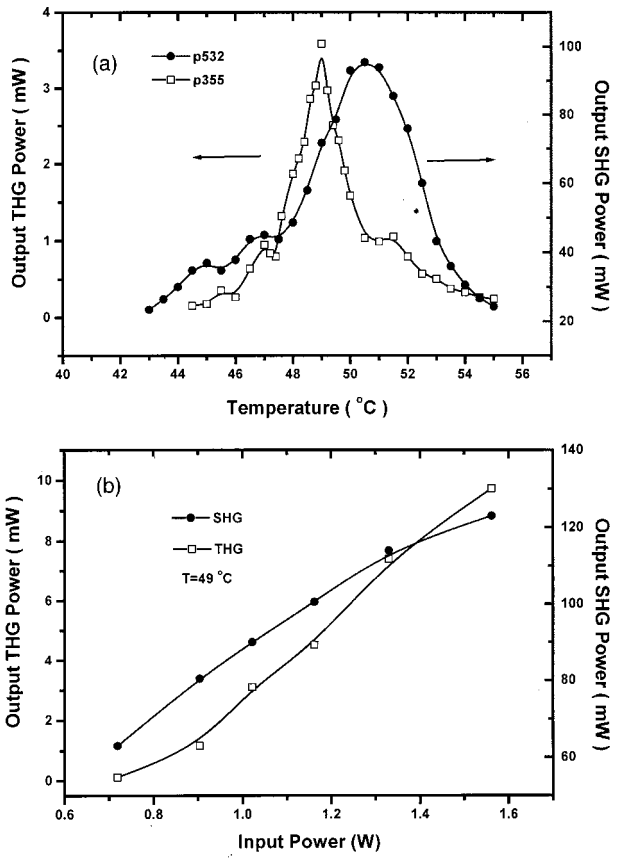

Fig. 9. (a) Average powers of SH and TH fields versus tuned temperature. The average power of the fundamental field is 1.1 W. (b) Average powers of SH and TH fields versus average power of the fundamental field. The sample temperature is constant at 39 °C.

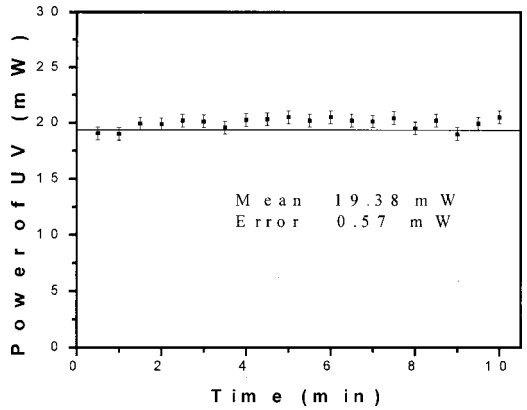

Fig. 10. Temporal behavior of the UV light output during a 10-min period.

temperature is not a perfect phase-matching temperature for SHG, the SHG power at this fundamental power level is just 120 mW, i.e., lower than 300 mW at 50.5 °C.

The measured THG efficiency is far below the theoretical value estimated by solution of the coupled equations with fundamental depletion. The reasons may be as follows: First, the peak temperatures of SHG and THG did not overlap, which indicates that the QPM conditions for frequency doubling and frequency adding were not perfectly satisfied simultaneously the measured sample. At the peak temperature during THG the efficiency of SHG was ~8% for the same measurement conditions. Because the SF efficiency is in proportion to the intensity of the SH, there was a sharp decrease in THG efficiency from that expected. Second, because the phase-matched temperature for the superlattice is 50 °C, the photorefractive effect in the short-wavelength region was still strong for the LT crystal, which resulted in changes in refractive index and in degradation of laser beam quality inside the crystal directly at the fundamental power level given above. Therefore the phase mismatches and conversion efficiency decreased.

To avoid the influence of the photorefractive effect, we redesigned the structure parameters and made the phase matching temperature for the new structure near 100 °C. A 21-mW UV output was obtained for 758-mW average fundamental power with an internal conversion efficiency of ~2.8%. The output was fairly stable throughout the whole experiment, which lasted for 2 h. No obvious degradation was observed. A temporal UV trace recorded for 5 min at an output power of ~19 mW is shown in Fig. 10. Measurements were made at 30-s intervals. The relative standard deviation was ~2.9%. These results demonstrate that the photorefractive effect is negligible at the operating temperature and power level.

5. CONCLUSIONS

We have presented a new kind of dual-periodic superlattice that can be used in various coupled optical parametric processes and have illustrated the designation of a frequency tripler that uses this structure. An optical $LiTaO_3$ superlattice with a dual-periodic domain-reversal structure was fabricated and tested. The structure achieved third-harmonic generation at 355 nm by tripling of an all-solid-state quasi-cw 1064-nm Nd:YVO_4 laser in a cascaded quasi-phase-matching scheme. Theoretically, the scheme has a higher efficiency and should produce a simpler light path for frequency tripling than a traditional scheme in which two bulk crystals or periodic superlattices are used in series. Owing to its greater feasibility for material design, the dual-periodic superlattice may have potential applications in many frequency-conversion devices.

ACKNOWLEDGMENTS

This research is supported by a grant from the State Key Program for Basic Research of China, from the National Advanced Materials Committee of China, and from the National Natural Science Foundation of China (10021001). S. N. Zhu is thankful for support from a monogrant RFPP.

S.-N. Zhu's e-mail address is zhusn@nju.edu.cn; telephone, 86-25-3593355; fax, 86-25-3595535.

REFERENCES

1. J. A. Armstrong, N. Bloembergen, J. Ducuing, and P. S. Pershan, "Interactions between light waves in a nonlinear dielectric," Phys. Rev. **127**, 1918–1939 (1962).
2. P. A. Franken and J. F. Ward, "Optical harmonics and nonlinear phenomena," Rev. Mod. Phys. **35**, 23–39 (1963).
3. M. Yamada, N. Nada, M. Saitoh, and K. Watanabe, "First-order quasiphased matched $LiNbO_3$ waveguide periodically poled by applying an external field for efficient blue second-harmonic generation," Appl. Phys. Lett. **62**, 435–436 (1993).
4. R. G. Batchko, M. M. Fejer, R. L. Byer, D. Woll, R. Wallenstein, V. Y. Shur, and L. Erman, "Continuous-wave quasi-phase-matched generation of 60 mW at 465 nm by single-pass frequency doubling of a laser diode in backswitch-poled lithium niobate," Opt. Lett. **24**, 1293–1295 (1999).
5. M. Fujimura, T. Suhara, and H. Nishihara, "Periodically domain-inverted $LiNbO_3$ for waveguide quasi-phase matched nonlinear optic wavelength conversion devices," Mater. Sci. B **22**, 413–420 (1999).
6. K. Koch and G. T. Moore, "Singly resonant cavity-enhanced frequency tripling," J. Opt. Soc. Am. B **16**, 448–459 (1999).
7. M. Fujimura, A. Shiratsuki, T. Suhara, and H. Nishihara, "Wavelength conversion in $LiNbO_3$ waveguide difference-frequency generation devices with domain-inverted gratings fabricated by voltage application," Jpn. J. Appl. Phys. **37**, L659–L662 (1998).
8. L. E. Myers, R. C. Eckardt, M. M. Fejer, R. L. Byer, W. R. Bosenberg, and J. W. Pierce, "Quasi-phase-matched optical parametric oscillators in bulk periodically poled $LiNbO_3$," J. Opt. Soc. Am. B **12**, 2102–2116 (1995).
9. M. A. Arbore, O. Marco, and M. M. Fejer, "Pulse compression during second-harmonic generation in aperiodic quasi-phase-matching gratings," Opt. Lett. **22**, 865–867 (1997).
10. C. B. Clausen, O. Bang, and Y. S. Kivshar, "Spatial solitons and induced Kerr effects in quasi-phase-matched quadratic media," Phys. Rev. Lett. **78**, 4749–4752 (1997).
11. S. N. Zhu, Y. Y. Zhu, and N. B. Ming, "Quasi-phase-matched third-harmonic generation in a quasi-periodic optical superlattice," Science **278**, 843–846 (1997).
12. S. N. Zhu, Y. Y. Zhu, Y. Q. Qin, H. F. Wang, C. Z. Ge, and N. B. Ming, "Realization of second harmonic generation in a Fibonacci optical superlattice of $LiTaO_3$," Phys. Rev. Lett. **78**, 2752–2755 (1997).
13. K. F. Kashi and A. Arie, "Multiple-wavelength quasi-phase-matched nonlinear interactions," IEEE J. Quantum Electron. **35**, 1649–1655 (1999).
14. Y. B. Chen, C. Zhang, Y. Y. Zhu, S. N. Zhu, H. T. Wang, and N. B. Ming, "Optical harmonic generation in a quasi-phase-matched three-component Fibonacci superlattice $LiTaO_3$," Appl. Phys. Lett. **78**, 577–579 (2001).
15. C. B. Clausen, Y. S. Kivshar, O. Bang, and P. L. Christiansen, "Quasiperiodic envelope solitons," Phys. Rev. Lett. **83**, 4740–4743 (1999).
16. X. J. Liu, Z. L. Wang, J. Wu, and N. B. Ming, "Second-harmonic generation in a Thue–Morse optical superlattice," Chin. Phys. Lett. **15**, 426–428 (1998).
17. X. J. Liu, Z. L. Wang, X. S. Jiang, J. Wu, and N. B. Ming, "Characterization of harmonic generation in an intergrowth optical superlattice," J. Phys. D **31**, 2502–2506 (1998).
18. B. Y. Gu, B. Z. Dong, Y. Zhang, and G. Z. Yang, "Enhanced harmonic generation in aperiodic optical superlattices," Appl. Phys. Lett. **75**, 2175–2177 (1999).
19. O. Pfister, J. S. Wells, L. Hollberg, L. Zink, D. A. Van Baak, M. D. Levenson, and W. R. Bosenberg, "Continuous-wave

frequency tripling and quadrupling by simultaneous three-wave mixings in periodically poled crystals: application to a two-step 1.19–10.71-μm frequency bridge," Opt. Lett. **22**, 1211–1213 (1997).
20. C. Zhang, H. Wei, Y. Y. Zhu, H. T. Wang, S. N. Zhu, and N. B. Ming, "Third-harmonic generation in a general two-component quasi-periodic optical superlattice," Opt. Lett. **26**, 899–901 (2001).
21. C. Zhang, Y. Y. Zhu, S. X. Yang, Y. Q. Qin, S. N. Zhu, Y. B. Chen, H. Liu, and N. B. Ming, "Crucial effects of coupling coefficients on quasi-phase-matched harmonic generation in an optical superlattice," Opt. Lett. **25**, 436–439 (2000).
22. S. N. Zhu, Y. Y. Zhu, Z. Y. Zhang, H. Shu, H. F. Wang, J. F. Hong, C. Z. Ge, and N. B. Ming, "$LiTaO_3$ crystal periodically poled by applying an external pulsed field," J. Appl. Phys. **77**, 5481–5483 (1995).
23. V. Y. Shur, E. L. Rumyantsev, E. V. Nikolaeva, E. I. Shishkin, D. V. Fursov, R. G. Batchko, L. A. Eyres, M. M. Fejer, and R. L. Byer, "Nanoscale backswitched domain patterning in lithium niobate," Appl. Phys. Lett. **76**, 143–145 (2000).